25 Secondary Flow and Channel Changes around a Bar in the Brahmaputra River, Bangladesh

W.R. ROY RICHARDSON, COLIN R. THORNE
Department of Geography, The University of Nottingham, University Park, Nottingham, NG7 2RD, UK

SALEEM MAHMOOD
FAP-24, House 96, Road 23, Banani, Dhaka, Bangladesh

ABSTRACT

This paper reports preliminary results and interpretations based on direct measurements of primary velocities, secondary currents, sediment concentrations and channel changes in the braided Brahmaputra (Jamuna) River in Bangladesh. Measurements were made around a braid bar using an Acoustic Doppler Current Profiler (ADCP) to measure velocity profiles and relative variations in suspended sediment concentration, with position fixing via a Differential Global Positioning System. A total of 16 transects were investigated during the 1994 summer monsoon runoff. In this preliminary review, data for two sections are examined to characterize the flow patterns in a curved anabranch alongside the bar and at the bifurcation just upstream of the bar.

Results demonstrate linkages between large-scale secondary flow cells, primary isovel distributions and pathways of concentrated suspended sediment transport. Along the flanks of the braid bar curved anabranch flow exhibits helical flow in the talweg, outward flow over the bar at the inner margin and, possibly, a counter-rotating secondary cell close to the outer bank. Plunging flow near the outer bank brings fast, relatively sediment-free water close to the bank toe, promoting scour, instability and bank retreat. Near-bed convergence and upwelling at the crest of the bar at the inner bank concentrates sediment, promoting deposition and bar growth. These patterns are similar to those observed in meander bends of single-thread rivers. At the flow bifurcation, flow exhibits an incremental shifting of helical flow in both halves of the channel driven by the changing distribution of flow approaching the study section. This process, together with the stage-related scour and fill patterns observed, gave rise to the growth of a medial bar along the channel centreline, where secondary flow converged.

This study demonstrates the utility of ADCP for investigations of flow and sediment transport distributions in rivers. An understanding of the distributions of flow and sediment movement may be used to explain observed patterns of bed scour and fill that are, in turn, responsible for short-term morphological developments. Examination of satellite images demonstrates that such short-term developments can only be properly understood within the context of channel planform evolution at larger spatial and temporal scales. It is further shown how developments at the bifurcation produce changes in the relative dominance of the anabranches, leading to evolution of the braided planform.

Coherent Flow Structures in Open Channels.
Edited by P.J. Ashworth, S.J. Bennett, J.L. Best and S.J. McLelland.

INTRODUCTION

During the 1994 summer monsoon in Bangladesh a joint study was undertaken between the University of Nottingham and Flood Action Plan 24 – The River Survey Project (FAP-24). This was one of a number of special studies performed under FAP-24 with the aim of improving our understanding of river morphology. The specific objectives of the study are to measure primary and secondary flow distributions around a bifurcation-bar-confluence unit and to investigate the extent to which the pattern of primary isovels, pathways of sediment transport and changes in channel morphology are influenced by secondary flow structures. While good progress is being made towards these objectives, data processing is on-going and, therefore at present, only preliminary results are available for publication.

SECONDARY FLOWS IN MEANDERING RIVERS

Secondary flows may be defined as velocities in the plane perpendicular to the axis of primary flow (Prandtl, 1952). Two types of secondary flow are generally recognized, stress-induced or weak secondary currents, caused by non-uniform distribution of boundary shear stress, and skew-induced or strong secondary currents, caused by skewing of cross-stream vorticity into a streamwise direction due to channel curvature or bed topography (Perkins, 1970). Generally, in rivers it is found that secondary flow patterns are dominated by skew-induced currents (Bathurst, 1979; Bathurst *et al.*, 1979; see Rhoads, this volume), however, planform morphology, channel shape and the distribution of bed roughness are important factors in determining the strength and form of secondary flow.

Research in meandering rivers has established that the pattern of primary isovels and pathways of bed material transport (both bedload and suspended load) are strongly affected by skew-induced secondary currents (Engelund, 1974; Hey & Thorne, 1975; Bathurst *et al.*, 1977; Bridge, 1977, 1984; Bathurst *et al.*, 1979; Dietrich *et al.*, 1979; Thorne & Rias, 1984; Thorne *et al.*, 1985; Odgaard & Berg, 1988; Markham & Thorne, 1992). Surface convergence and plunging flows convect fast, near-surface water towards the solid boundary, promoting a steep near-bed primary velocity gradient, high local boundary shear stresses and bed scour. Conversely, convergent secondary flow near the bed causes upwelling of slow, near-bed flow, promoting deposition. Sediment concentrations are also affected by secondary flows. Plunging flow brings near-surface water that is relatively sediment free into proximity with the boundary, where it can pick-up sediment to cause scour. Upwelling carries sediment laden, near-bed water higher into the water column, where primary velocities sweep it along as a sediment plume. Such plumes have been observed to link sediment sources to sediment deposition zones in alluvial rivers (Peters, 1977; Peters & Goldberg, 1989). Secondary currents are known to occur at all flow stages in meander bends (Markham & Thorne, 1992) and at high flow they may persist through the inflexion point between meanders

(Thorne & Hey, 1979).

In a study of the Fall River, USA (Thorne *et al.*, 1985) measurements were made in meander bends at low, intermediate and bankfull stages. Figure 25.1 shows results for a section close to a bend apex at bankfull flow that are similar to those of several other studies (Hey & Thorne, 1975; Bathurst *et al.*, 1977; Bridge, 1977, 1984; Bathurst *et al.*, 1979; Thorne & Rias, 1984).

The main feature of the secondary flow is a helical, skew-induced cell which carries fast surface-water towards the outer bank and slower near-bed water towards the inner bank. However, a small cell of reverse rotation is also present at the outer bank. This cell occupies the channel between one and two times the bank height away from the outer bank. It is caused by local interaction of the skew-induced cell with the steep outer bank (Bathurst *et al.*, 1979). The skew-induced and outer-bank cells combine to depress the maximum primary velocity core below the water surface and compress primary isovel spacing close to the bank toe (Figure 25.1). This leads to toe scour that erodes and destabilizes the outer bank, and which quickly removes bank-failure debris to promote rapid bank retreat (Thorne & Lewin, 1979).

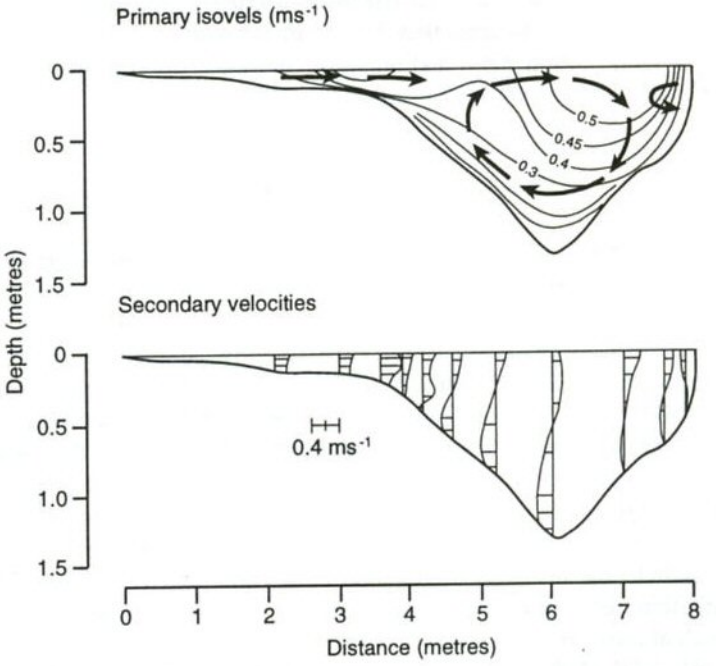

Figure 25.1. Primary isovels and secondary velocity profiles for bankfull flow at a meander apex on the Fall River, USA. Note that secondary arrows superimposed on primary isovels are inferred from isovel curvature and measured horizontal secondary velocities. (after Thorne *et al.* 1985)

Flow over the point bar in Figure 25.1 is directed radially outwards over the whole flow depth, corroborating the work of Dietrich *et al.* (1979). There are two reasons for outward flow. First, the flow area is decreasing in the downstream direction over the point bar, causing water to be directed outwards (topographically steered) to maintain continuity. Second, at the inner bank the outward acting centrifugal force, due to the channel curvature, overcomes the inward acting pressure gradient force, due to super-elevation, carrying water outwards over the point bar (Dietrich, 1982; Dietrich & Whiting, 1989). This pattern of flow leads to convergence of near-bed flow and strong upwelling where the skew-induced cell meets the zone of outward flow. The morphology of the bar is moulded by the secondary pattern to display a flat upper point bar platform dominated by outwards flow, a steep point bar face dominated by inwards flow and a sharp point bar crest beneath the zone of upwelling at the junction of the two secondary flow features. Growth of the point bar occurs through advance of the bar crest towards the retreating outer bank. This drives bend growth and migration that is typical of meandering rivers (Friedkin, 1945; Thorne & Lewin, 1979; Lapointe & Carson, 1986; Thorne, 1991).

Qualitative descriptions and explanations of secondary current patterns in single-thread meandering channels have proved to be a crucial prerequisite to successful mathematical modelling, because they have clarified which terms in the governing equations of fluid motion may, and may not, be neglected (Dietrich & Whiting, 1989; Smith & McLean, 1984, Odgaard & Berg, 1988).

SECONDARY FLOWS IN BRAIDED RIVERS

There have been few field measurements of velocity fields around bars in braided rivers, with those of Bridge & Gabel (1992) being an exception. To date there has been no systematic, field-based study of secondary currents in a large, sand-bed braided river. Bristow & Best (1993) have recently presented a comprehensive review of past studies. They found that field work has tended to emphasize flow and morphological dynamics at confluences, while the link between converging flow at a confluence and subsequent divergence, leading to bifurcation of the channel, has been relatively neglected. Consequently, rather little is known about flow patterns in large braided rivers (Peters, 1977) and even less about any role secondary currents may play in confluence-diffluence mechanics (Best & Bristow, 1993). Similarities between meandering and braided rivers do exist, however, (Thorne *et al.*, 1993) suggesting that secondary currents could be in part responsible for significant morphological forms in braided rivers.

Ashworth *et al.* (1992) suggested that a bifurcated channel could be viewed as consisting of back-to-back meander bends (Figure 25.2a), the left channel being a mirror image of the right. On this basis, they suggested that the secondary flow pattern would consist of twin skew-induced cells, diverging at the surface and

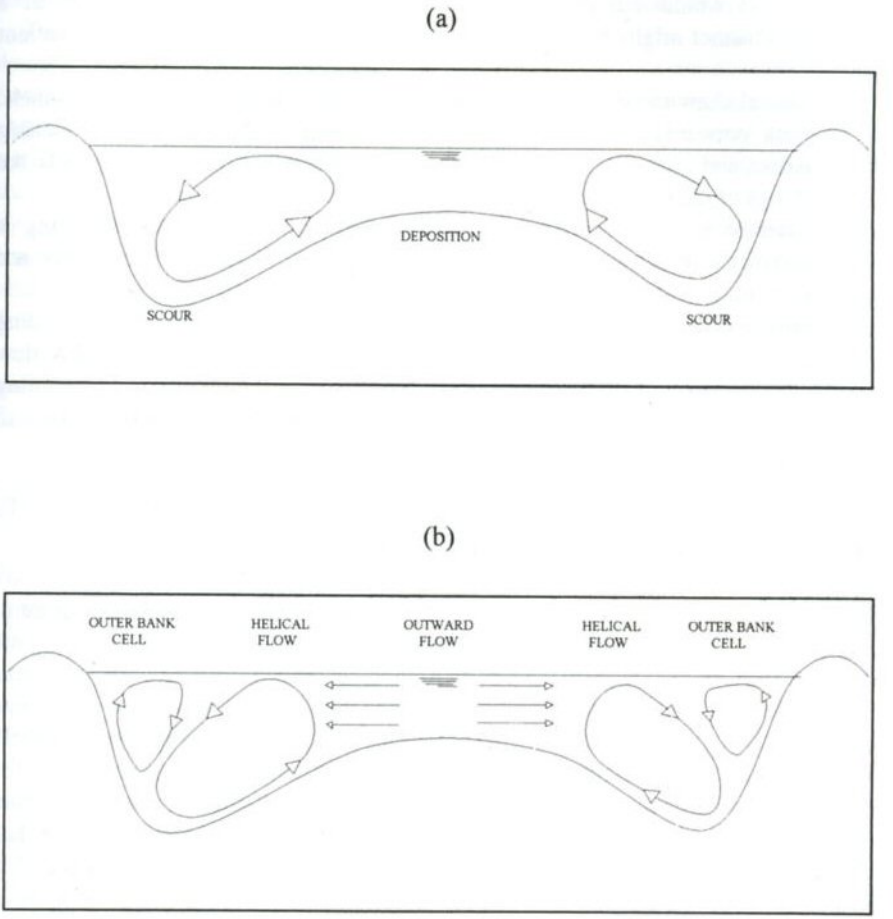

Figure 25.2. (a) Concept of secondary flow in a bifurcated channel as a mirror image of two meanders (after Ashworth *et al.*, 1992); (b) Concept of secondary flow in a bifurcated channel proposed in this study

converging at the bed (Figure 25.2a). The resulting circulation drives fast surface water outwards to the banks where it plunges, and brings slow, near-bed water inwards, where it upwells at the channel centre.

While the analogy of a bifurcated channel in a braided river with back-to-back meanders has merit, examination of the results reported in the previous section on flow in meander bends of single-thread channels suggests that the concept of secondary current cells in Ashworth *et al.* (1992) possibly over-simplifies the situation found in nature.

A mirror image of the current understanding of secondary flow at a meander bend (Figure 25.1) would indicate that the likely pattern of secondary currents in a bifurcated channel might be similar to that shown in Figure 25.2b. The salient features are:

- helical skew-induced flow confined to the deep anabranch talweg channels, with outwards flow driving fast surface water towards the outer, eroding banks and inwards flow bringing sediment laden near-bed flow towards the flanks of the braid bar;
- outer-bank cells generating surface convergence, with flow plunging a distance one or two times the bank height away from the outer banks and promoting basal scour and undercutting around the bank toe; and
- outward flow over the upper braid bar at the channel centre, concentrating bed material transport and deposition at the near-bed flow convergence/upwelling zone on the flanks of the braid bar and promoting deposition of fine sediment on the bar top through reducing velocity and unit discharge over the bar in the downstream direction.

THE BRAHMAPUTRA RIVER, BANGLADESH

The Brahmaputra is one of the world's largest rivers with a mean daily discharge of 19 600 $m^3 s^{-1}$, a mean annual peak discharge of 65 500 $m^3 s^{-1}$ and a total sediment load of the order of 500×10^6 tonnes per year (Coleman, 1969; Barua, 1994). The flow regime is strongly seasonal, with the great majority of flow occurring during the summer due to Himalayan snowmelt and monsoonal rainfall. The river discharge usually peaks in late July or early August. In 1988 the monsoon flood had a peak discharge of 98 600 $m^3 s^{-1}$ and an estimated return period of 65 years (Brammer, 1990). Measurements of discharge over the last 37 years show no discernible change in the annual maximum discharge (Sir William Halcrow & Partners Ltd., 1993) suggesting that the hydrological regime is steady, at least over engineering time-scales.

The main tributaries of the Brahmaputra River are the Teesta, Dudhkumar and Dharla rivers, each of which contributes a large volume of sediment derived from the southern flanks of the Himalayas. There are two important distributaries, both on the left bank (Figure 25.3). One of these, the Old Brahmaputra, is actually a former course of the main river, abandoned in the late 18th Century. The river downstream of the Old Brahmaputra offtake is called the Jamuna in Bangladesh.

The channel of the Brahmaputra is braided and its dominant morphological features are multiple anabranches separated by bars and islands. Coleman (1969), Bristow (1987) and Thorne *et al.* (1993) have established that there are two distinct braid bar levels. First order bars (islands) are of the order of 30 km in length and are scaled on the width of the primary channel. These islands have surface elevations close to floodplain level and are only partially submerged at bankfull flow. Second

order bars (braid bars) are of the order of 6 km long and are scaled on the width of the major anabranches. These bars are completely submerged at bankfull flow.

The islands are vegetated, inhabited and persist in about the same location for decades. They grow laterally by sand accretion when braid bars are attached to their flanks, and vertically by silt deposition during over-bank flows, giving them a characteristically layered stratigraphy (Bristow, 1987). They erode when attacked by curving anabranches on one or both sides (Bristow, 1987; Thorne *et al.*, 1993). The second order braid bars are much more mobile and are continually being re-worked by the river. Bars grow and migrate downstream through erosion around the bar head coupled to sand deposition on the flanks and bar tail and their dynamics are related to seasonal stage changes in the main anabranches (Bristow, 1987; Bristow & Best, 1993). On the basis of their high mobility, rapidity of adjustment to imposed flow conditions and close association with the hydraulics of the major anabranches, the second-order braid bars were selected as the appropriate scale for the field measurements of this study.

FIELD STUDY

To investigate the patterns of secondary flow, sediment concentration and channel change, measurements around a bifurcation-bar-confluence unit were made during the summer monsoon in 1994. The study site was selected following a reconnaissance survey in May 1994. It encompasses a bar in the left-bank anabranch of the Brahmaputra, 10 km south of Bahadurabad (Figures 25.3 and 25.4). At the beginning of the field study, in May 1994, the left sub-channel flanking the bar was dominant, carrying approximately three times the flow of the right sub-channel. However, during 1994 the right sub-channel grew at the expense of the left, so that at the end of the survey period in November 1994, the sub-channels were of about equal size.

In the survey 16 transect lines were established, starting 5 km upstream of the study bar and continuing downstream of the bar (Figure 25.4). In this preliminary paper consideration is limited to results from Sections 3 and 6. These transects were selected to represent flow in two key areas: the curved sub-channel alongside the bar, and; the point of bifurcation upstream of the bar head. Measurements were made from the main vessel of the River Survey Project, using a 300 kHz Acoustic Doppler Current Profiler (ADCP) and dual frequency echo-sounder. Measurements were made in May, August and September 1994 corresponding to the rising, peak and falling stages of the monsoon event. Use of a differential global positioning system (DGPS) for position fixing meant that errors in relocating transects were of the order of ±5 m, which is negligible in an anabranch over 500 m wide.

An ADCP uses the Doppler effect to measure three-dimensional velocity profiles. It should be noted that the ADCP cannot measure velocities at the bed. The Doppler effect is the change in apparent sound pitch that results from relative

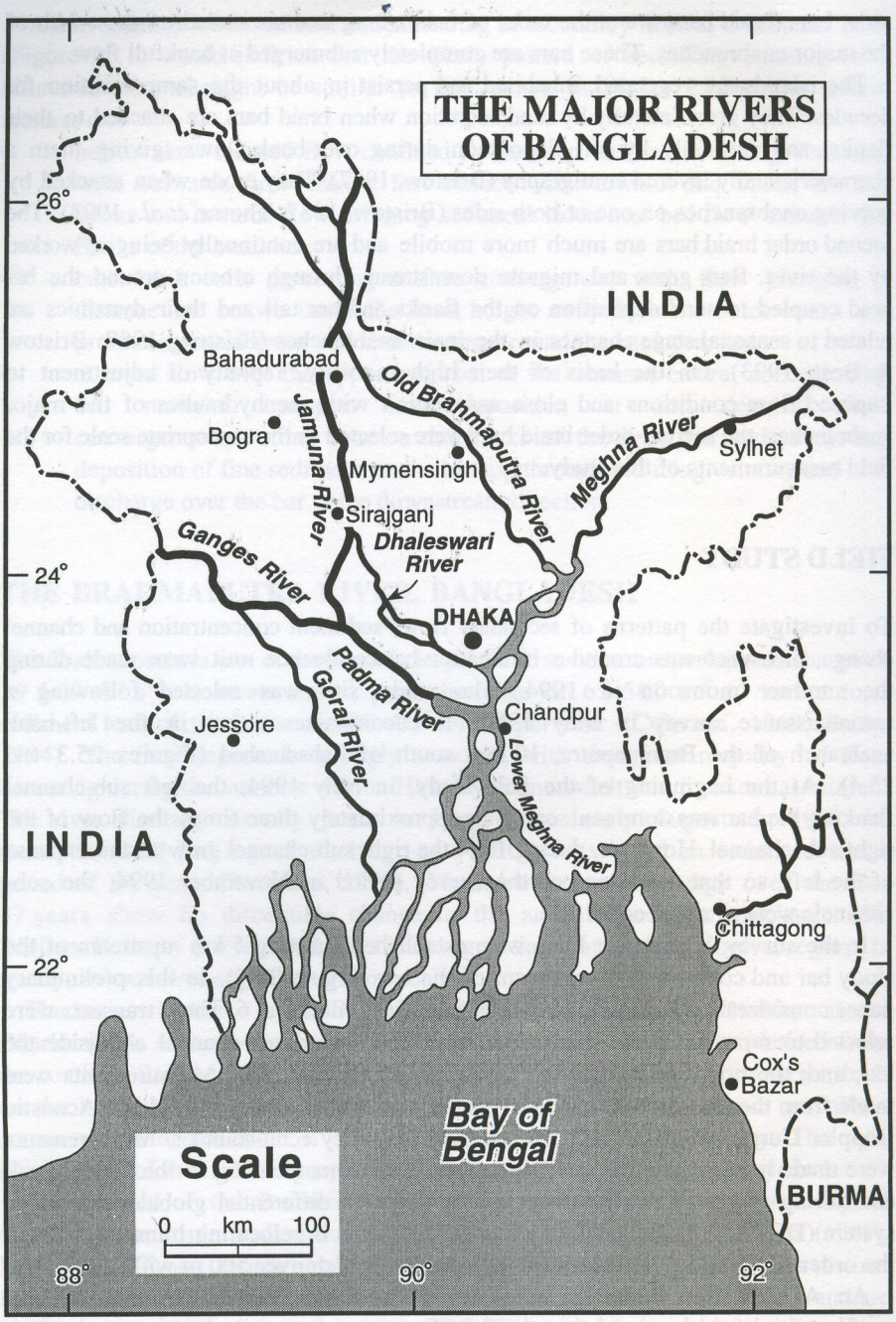

Figure 25.3. The major rivers of Bangladesh. Study site is just south of Bahadurabad on the Jamuna River

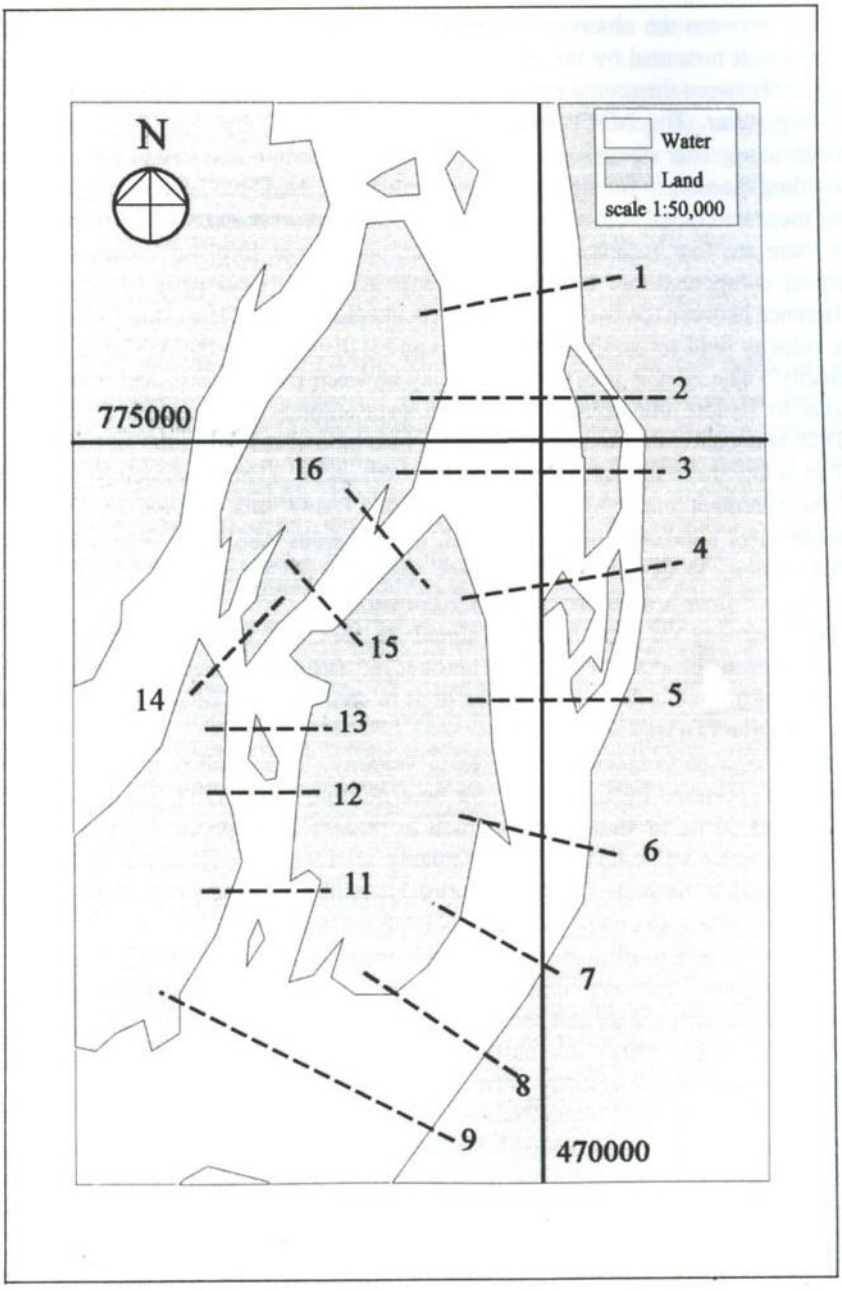

Figure 25.4. Map of study bar and transect lines used in the field survey based on LANDSAT image for 1994. Co-ordinates refer to transverse Mercator system for Bangladesh. Only results for Sections 3 (bifurcation) and 6 (curved sub-channel) are discussed here

motion between the observer and the source. The magnitude of Doppler shift in sound pitch measured by the ADCP is directly proportional to the relative radial velocity between the source and sound scatterers such as suspended sediment in the flowing water. The ADCP measures velocity profiles by transmitting acoustic pulses along four diverging beams in the water column every 0.5 s and then recording the shift in frequency of the returned signals. The ADCP then resolves the four measured radial velocities into north-south, east-west and vertical components. As there are four measured velocities but only three resolved components, the vertical component can be calculated twice using different pairs of beams. The difference between the two calculated vertical velocities is due to non-uniformity of the velocity field across the sampled area and is displayed by the ADCP as an 'error velocity'. The ADCP uses the time delay between transmission and return of the signal to sample the velocity profile in measurement ranges (termed bins). The ADCP was configured to sample the data into bins of 0.5 m depth, extending from 2.7 m below the water surface to near the bed, and to average velocity profile data in measurement ensembles every 10 pings. Using this method of successive measurement onboard a moving vessel, a continuous data set is obtained for each cross-section. With an average vessel speed of 4 knots, the velocity profile represents a flow field approximately 10 m wide.

The intensity of the returned signal in decibels is also logged. This is approximately proportional to the amount of suspended material scattering the acoustic signal and, therefore, can be used to indicate relative suspended sediment concentration (Thorne *et al.*, 1994).

DGPS is used to calculate the vessel velocity. This enables correction of the velocities measured by the ADCP for boat motion. The DGPS has a positioning accuracy of ±1 m in static mode, which in practice corresponds to an error in the measured water velocities of approximately ±0.15 m s^{-1}. However, within each velocity profile the same DGPS correction is applied over the whole flow depth, so that no bias is introduced in plots of secondary currents.

Measured north-south and east-west velocities do not necessarily correspond to the primary and secondary components. There are a number of methods that may be used to define the primary and secondary planes and these were reviewed recently by McLelland *et al.* (1994). As outlined by McLelland *et al.* (1994) none of the traditional methods of velocity correction in open channels is suited to studies on large braided rivers such as the Brahmaputra.

Braided rivers are characterized by a multi-threaded planform. In any one cross-section in a braided channel there may be several talwegs separated by various bed features, which may contain a core of local maximum velocity acting as a semi-independent stream. It is proposed that each of these streams of water will have their own primary and hence secondary orthogonal velocity directions. Therefore, any technique for correcting velocity measurements in a braided river should be able to define separate secondary flow planes for each stream of water in a multi-threaded channel cross-section.

In order to achieve this goal a secondary flow function was derived to search for secondary flow activity for various alignments in a river channel. The proposed secondary flow function measures helical rotation for various cross-sectional alignments and highlights peaks at certain orientations. Taking the measured flow velocity components as velocity magnitude (V_H) and velocity direction (φ), and referring to the corrected velocity components as primary (U_P) and secondary (U_S), the secondary flow function is defined as:

$$\left(\frac{U_P}{|U_S|}\right)(y - Y)W$$

where $U_S = V_H \cos(\varphi - \alpha)$, α is the flow orientation, y is the depth of the measurement 'bin' being considered, Y is the average depth and W is the width of the measurement ensemble. For each velocity profile an average depth is calculated and then the above function is summed for all individual velocity measurements. The process is then repeated for all velocity profiles in a given cross-section and a value of the secondary flow function is obtained. All possible orientations (α = 0 to 180°) are then applied and a graph of the secondary flow function versus plane orientation is obtained (Figure 25.5a). A graph of the secondary flow function versus distance along the cross-section is then plotted for each value of plane orientation associated with a peak value of the secondary flow function (Figures 25.5b and 25.5c). Figures 25.5b and 25.5c can be used to determine which streams within the braided cross-section correspond to which plane orientation. The channel can then be sub-divided by locating the position of minimum depth average velocity between cores of local maximum velocity. Each stream of water can then be given a separate value of primary and secondary flow direction.

HISTORICAL PLANFORM CHANGES

The results of field measurements made during a single monsoon event must be interpreted in the context of longer term channel development at the study site. Historical LANDSAT satellite images covering the study area were supplied by Flood Action Plan 19 – Geographical Information Systems. Images were obtained from 1990, 1992, and 1994. The historical record of planform change was used to document and establish morphological changes around the study site over the medium term.

The recent record of planform developments in the left-bank anabranch of the Brahmaputra River (Figure 25.6) confirms that flow and channel change processes observed around a single bar during a single flow season can only be understood within the context of morphological changes at larger time and spatial scales. Figure 25.6 shows that the left-bank anabranch of the Brahmaputra River in 1990 is predominantly meandering with a sinuous alignment. There is a west-bank concave curve north of Bahadurabad and the future site of the study bar is at the

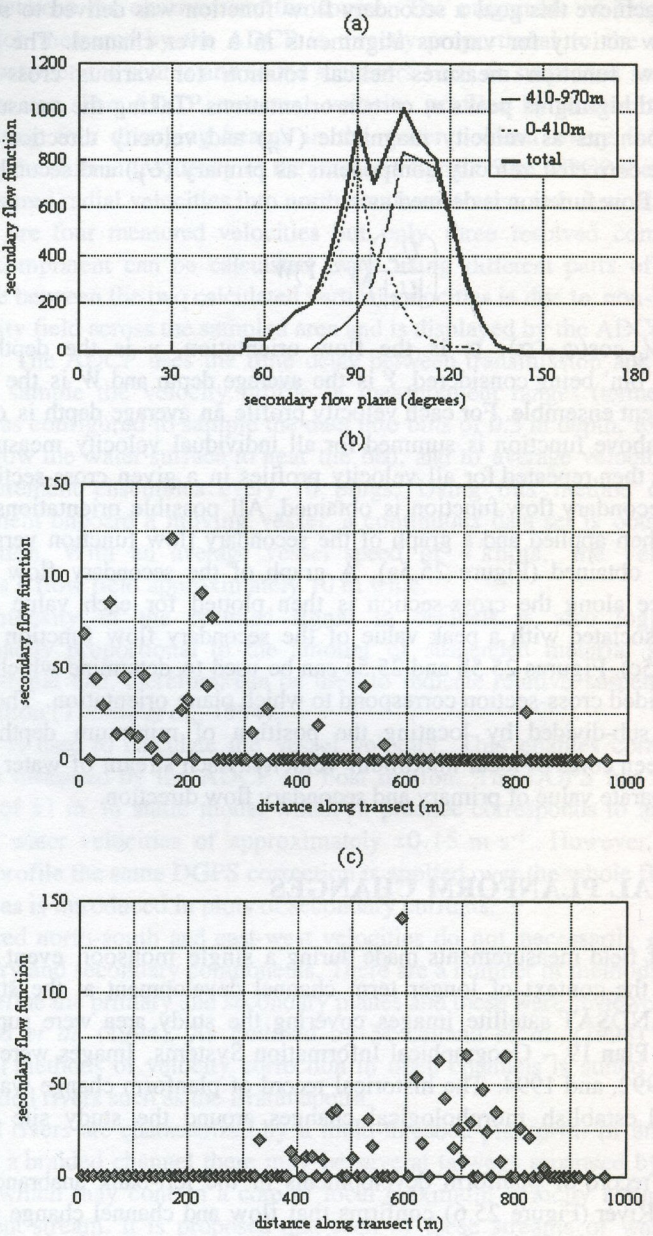

Figure 25.5. Velocity correction method applied to September data at section 3, (a) graph showing secondary flow function plotted against flow orientation; (b) and (c) graphs showing secondary flow function plotted against distance along transect for peak values of flow orientation shown in (a)

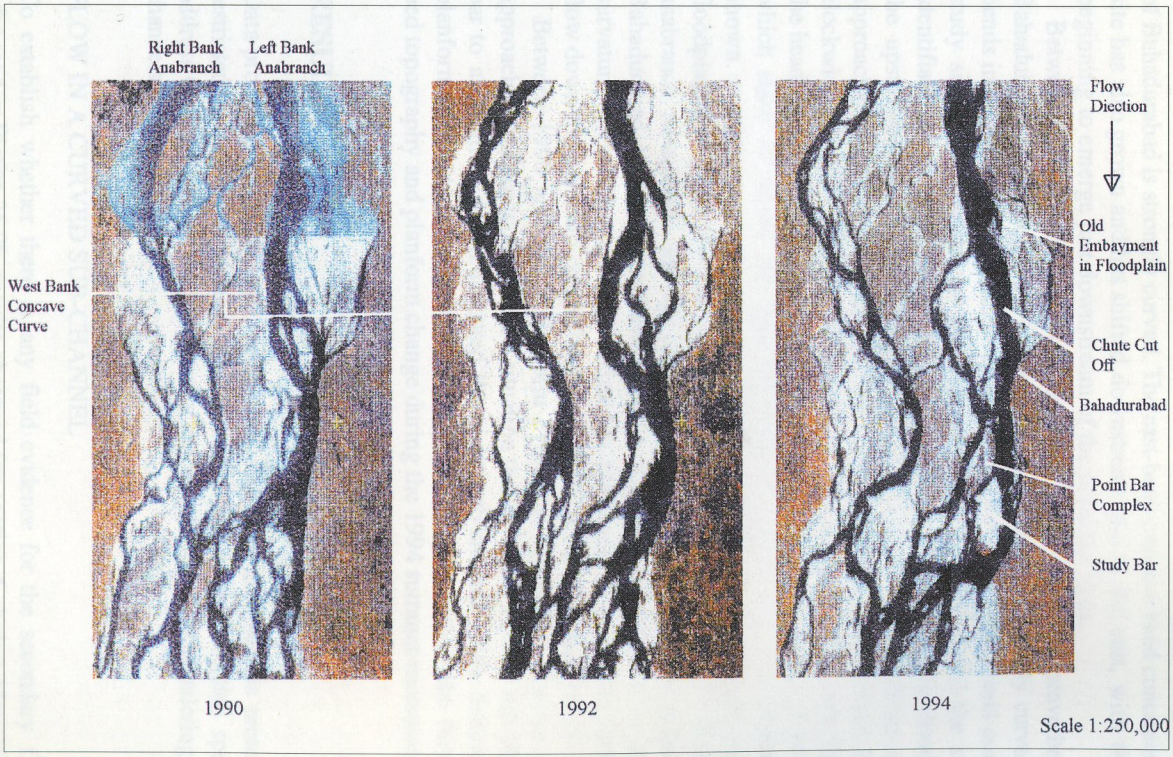

Figure 25.6. LANDSAT images for the Brahmaputra River around the study reach in 1990, 1992 and 1994. Yellow crosses may be used for cross-reference between images. Note increase in sinuosity of left-bank anabranch between 1990 and 1992 and cut-off north of Bahadurabad between 1992 and 1994. Flow orientation and curvature approaching the study bar are dependent on morphological changes immediately upstream

trailing edge of a growing point bar complex in an east-bank concave bend that is attacking the floodplain along the east-bank, south of Bahadurabad.

By 1992, the curves in the left-bank anabranch had grown in amplitude to give the left-bank anabranch a more sinuous course. The west-bank concave bend, north of Bahadurabad is strongly curved. The east-bank concave bend containing the study site has also grown and has shifted downstream and to the east, with the study bar beginning to emerge just downstream of the point bar apex.

Between 1992 and 1994 a chute cut-off of the west-bank concave bend north of Bahadurabad occurred. This is a common phenomenon for sharply curved anabranch bends in the Brahmaputra (Klaassen & van Zanten, 1989). The bend containing the study site has continued to grow and migrate downstream and the study bar is identifiable as the apex element of the point bar complex in this bend. However, the upstream cut-off has changed both the heading and curvature of the flow approaching the study reach. In 1992 the approach heading was about 140°, with a clockwise curvature which favoured the left sub-channel at the study bar. By 1994 the heading had changed to about 180°, and the planform curvature is anticlockwise, which starts to favour the right sub-channel. Historically, the Brahmaputra has shown a tendency to abandon and then re-occupy embayments cut into the floodplain by aggressive anabranch bends (Thorne *et al.*, 1993). If the left-bank anabranch re-occupies the old meander scar visible in the bank-line north of Bahadurabad, its heading will swing further to the south-west and its anticlockwise curvature will increase as it approaches the study area. This would further promote flow down the right sub-channel at the expense of the left sub-channel.

Between 1990 and 1994, planform evolution altered the heading of the flow approaching the study area from a situation that favoured the left sub-channel at the bar to a situation which favoured the right sub-channel. This demonstrates how planform evolution sets the scene for the changes observed in the flow structures, bed topography and planform change during the 1994 summer monsoon.

RESULTS

Data processing in this study is at an early stage and the analysis presented here is restricted to data for two transects. Sections 3 and 6 were selected specifically to address the issues raised in the review of secondary flows in meandering and braided channels presented earlier.

FLOW IN A CURVED SUB-CHANNEL

To establish whether there is any field evidence for the secondary flow pattern proposed in Figure 25.2b, results observed for section 6 during May 1994 are first considered. section 6 is located mid-way along the divided flow reach near the apex of the curve in the left sub-channel (Figure 25.4). Figure 25.7 shows plots of

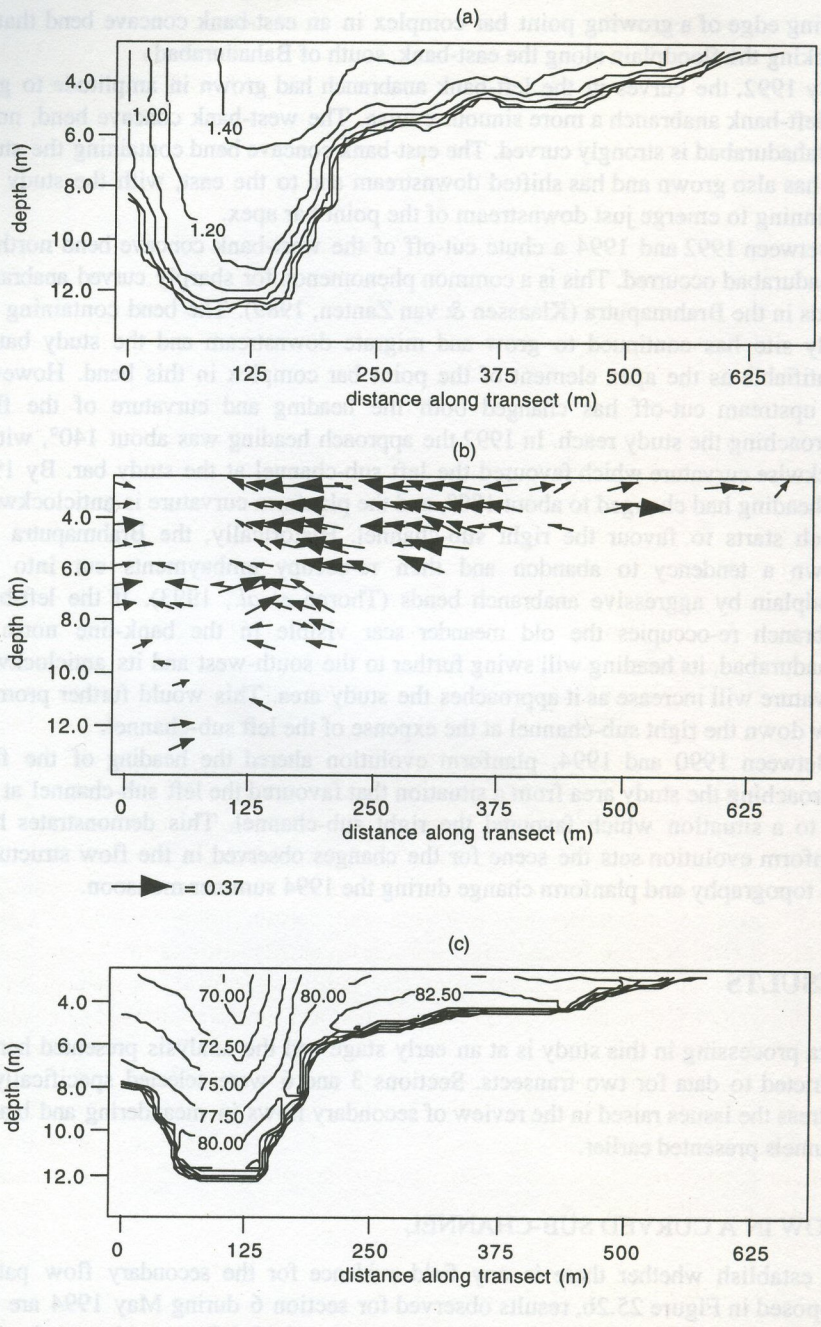

Figure 25.7. Results from section 6 for (a) primary isovels; (b) secondary velocities; and (c) ADCP backscatter from the May 1994 survey. Only significant secondary velocities are plotted (> 0.15 m s^{-1}) in cross-section (b)

primary isovels, secondary velocities and relative backscatter intensity.

Examination of the cross-sectional geometry shows that it displays morphological features similar to those found in a single-thread channel bend. The section is highly asymmetrical with deep scour close to the outer (east) bank and a well defined talweg channel, separated from a prominent bar at the inner bank by a sharp bar crest. The outer bank is known to be retreating from comparison of recent satellite images (Figure 25.6).

The primary isovels (Figure 25.7a) display a single core of maximum velocity above the talweg, with tightly packed isovels close to the bed at the bank toe and on the point bar. Primary isovels close to the outer bank near the water surface are more widely spaced. Above the point bar crest, upward bulging of the isovels suggests that there may be a zone of upwelling flow.

The plot of secondary velocities is consistent with this interpretation of the primary isovels. Helical circulation is evident in the talweg, with outward flow in the upper half of the profile and inward flow at depth. At the outer bank there is some evidence of an outer bank cell of reverse rotation in that secondary flow near the surface is directed inwards. The position and dimensions of the outer bank cell suggested by the secondary velocities coincide with the low velocity zone in the primary isovels and the zone of plunging flow is consistent with the area of closely packed isovels at the bank toe. At the point bar crest, secondary flow is directed radially outwards over the whole flow depth and a strong secondary velocity component can be seen to flow over the point bar crest to join the outwards surface flow of the helical cell in the talweg. Bed convergence and upwelling are evident on the point bar face. At the inner bank there is a zone of inward flow that may be indicative of a zone of flow separation (Markham & Thorne, 1992).

In Figure 25.7c the relative backscatter intensity plot at section 6 shows high sediment concentrations over the point bar platform, on the point bar face and close to the outer bank. These are areas of upwelling in the velocity measurements. There is an area of water with very low sediment concentration above the talweg, associated with the core of maximum primary velocity. Bulges in the isolines in Figure 25.7c are also consistent with the effects of upwelling evident in the primary velocity plot above the point bar crest and the secondary velocity plot at the point-bar face.

Taken together, the results for section 6 are consistent with patterns of primary velocity and secondary flow observed in bends of single-thread rivers (Figure 25.1) and display the elements hypothesized in Figure 25.2b. The backscatter results are also consistent with suspended sediment load measurements made in single-thread meander bends by Dietrich & Smith (1983).

FLOW AT A BIFURCATION

Figure 25.8 shows results for section 3 in May, August and September 1994, corresponding to rising, peak and falling monsoon flood stages. In May this section

was located near the flow bifurcation, immediately upstream of the study bar. During the course of the summer monsoon the nose of the study bar migrated approximately 0.5 km downstream while another, smaller medial bar formed in the left channel to the east. When applied to the data for May, the procedure to locate the primary and secondary planes for section 3 revealed two primary directions in the flow field, with headings of 80° for the flow between 0 and 787 m across the section and 98° between 787 and 1044 m across (Figure 25.8a). That is, the velocity streams are diverging by 18°. It should be noted that the results plotted in Figure 25.8a display primary and secondary velocities resolved according to the primary direction for each segment of the cross-section.

The plot of primary isovels for May shows two cores of maximum velocity, separated by a band of low velocity water between 700 and 900 m (Figure 25.8a). The larger core is associated with the flow direction in the channel between 0 and 787 m, which enters the left sub-channel. The smaller core is associated with the flow between 787 and 1044 m, which enters the right sub-channel. These results illustrate that although the cross-section is roughly parabolic, with no topographic divide in the channel bathymetry, the flow has already begun to bifurcate hydraulically.

The secondary velocities confirm that a hydraulic bifurcation has occurred, with markedly different secondary patterns in the two velocity streams. On the left side of the channel (250 to 600 m) the secondary velocities display clockwise helical circulation. This is a skew-induced cell associated with curvature of the flow as it approaches the study reach through a large, west-bank concave bend (see Figure 25.6, 1994 image). Close to the left-bank (0 to 250 m) secondary velocities are complex and difficult to interpret. In the right side of the channel (850 to 1044 m) secondary velocities are directed strongly to the right (west) over the whole flow depth. This is associated with topographic steering of the flow towards the right sub-channel. At this stage and location there is, apparently, insufficient curvature of flow entering the right sub-channel to generate a strong skew-induced secondary cell. Around the flow bifurcation (600 to 830 m) secondary velocities are generally weak and their directions are diverse, including significant vertical components. This suggests an area of complex, highly turbulent flow. In the field the water surface in this area displayed lines of boils and vortices typical of a turbulent shear layer.

The backscatter intensity plot shows a filament of water with a relatively low sediment concentration associated with area of flow bifurcation (700 to 830 m). In the field flow in the left sub-channel was observed to be eroding the flank of the bar close to the bar head. An area of high sediment concentration is displayed in the left channel associated with the zone of upwelling in the helical secondary flow of the left flow stream (300 to 450 m).

The results for high-stage flow in August are shown in Figure 25.8b. The procedure to locate the primary and secondary planes for this section again showed two primary directions in the flow field, with headings of 78° for the flow between

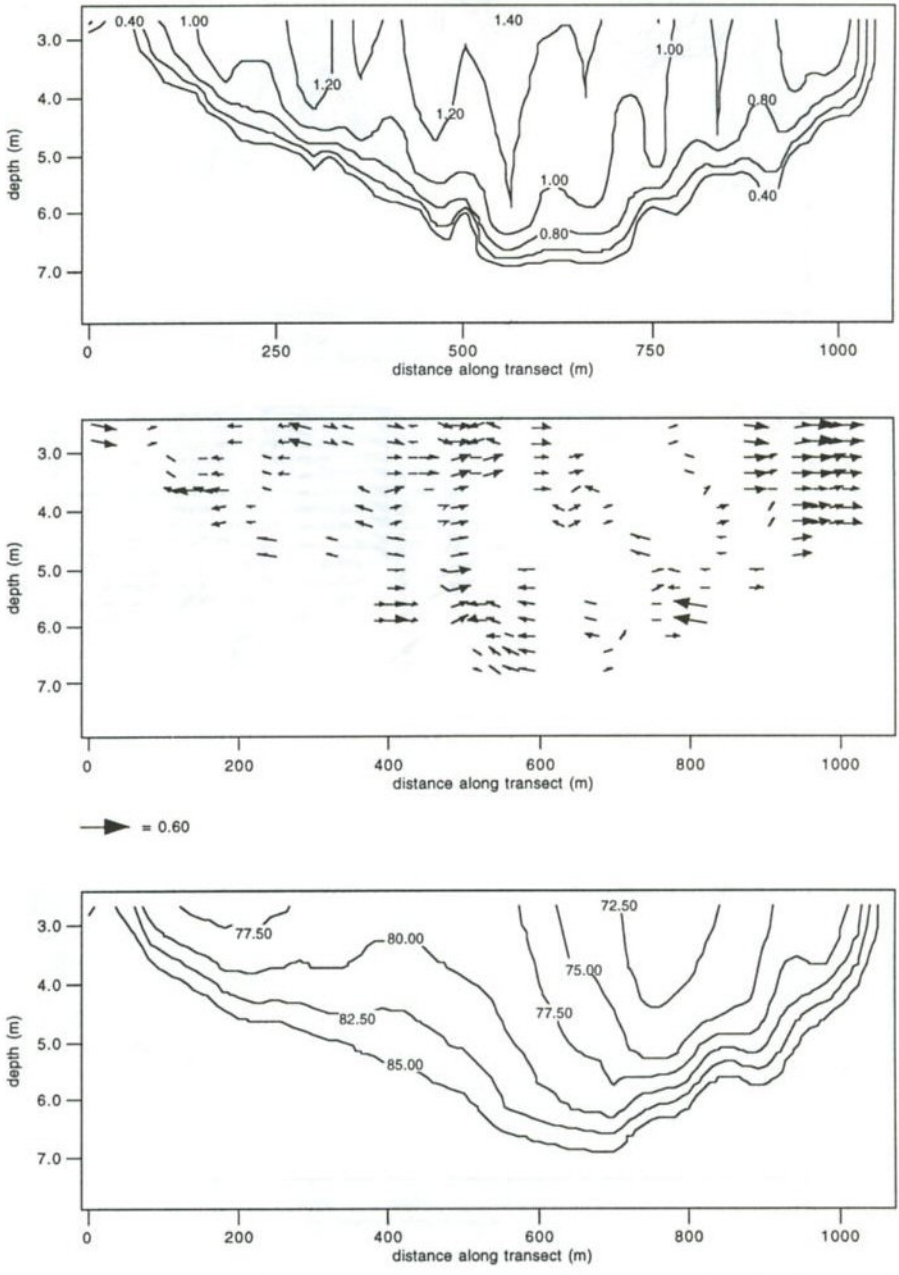

Figure 25.8. (a) Results from section 3 for primary isovels, secondary velocities and ADCP backscatter from May 1994. Only significant secondary velocities (> 0.15 m s^{-1}) are plotted. *Continued on next page*

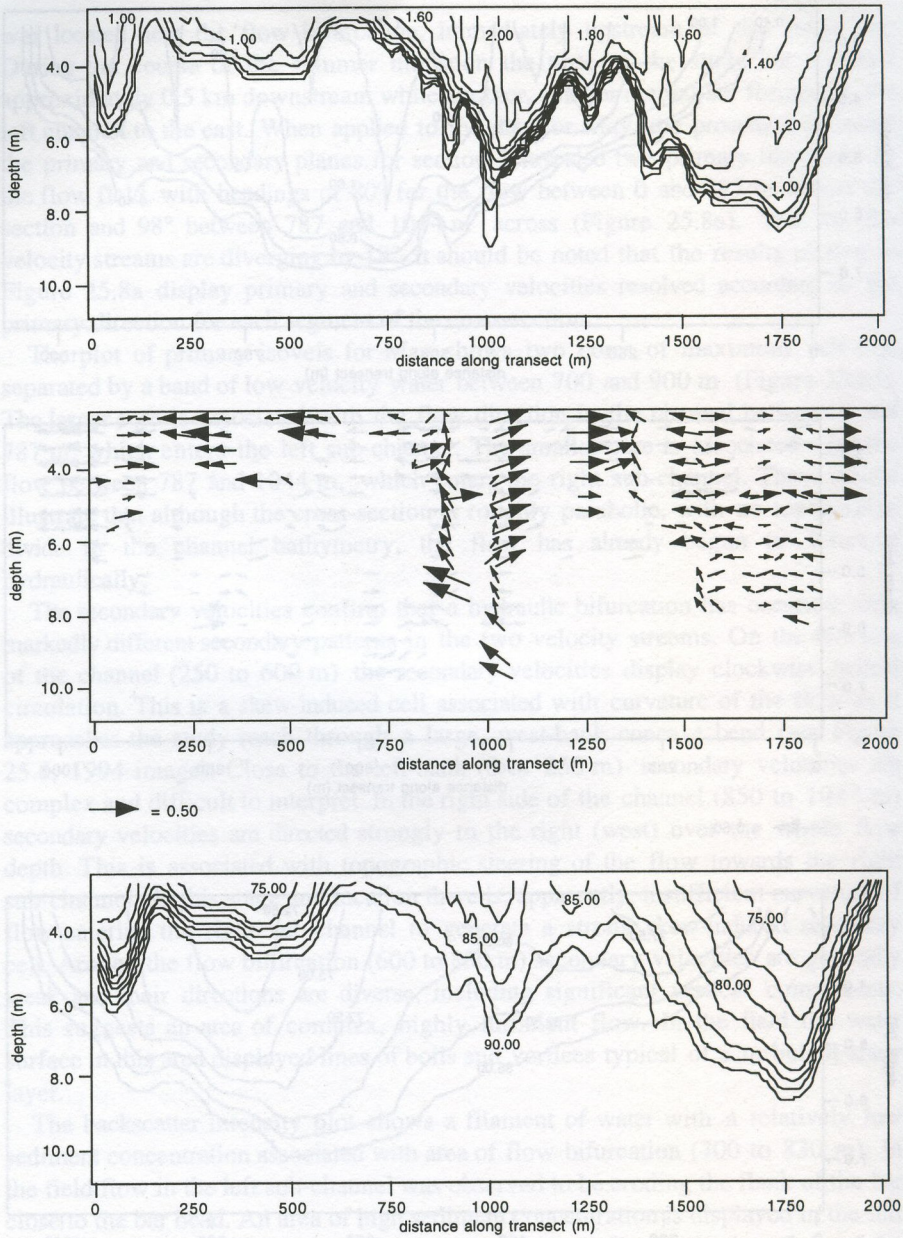

Figure 25.8. *continued* (b) Results from section 3 for primary isovels, secondary velocities and ADCP backscatter from August 1994. Only significant secondary velocities (> 0.15 m s^{-1}) are plotted. *Continued on facing page*

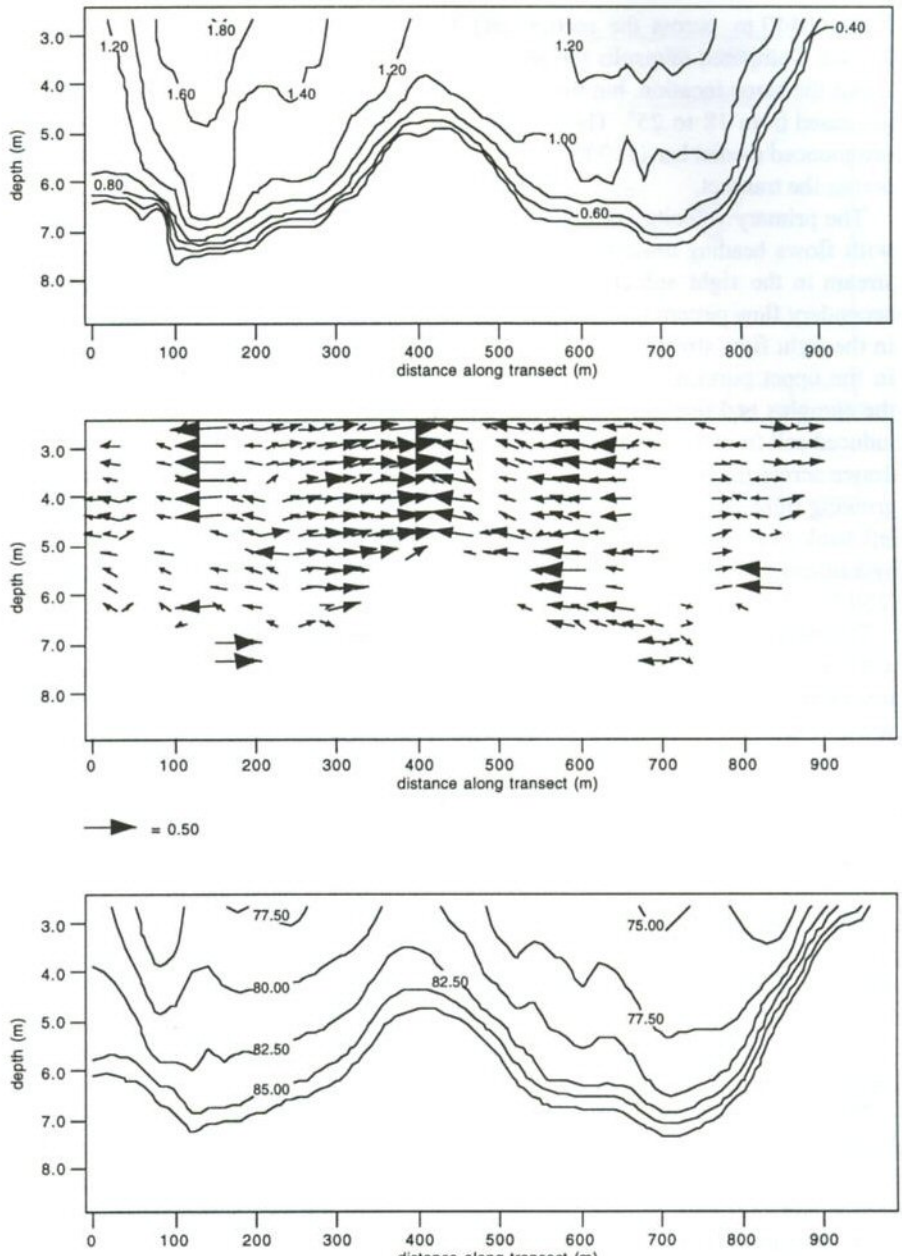

Figure 25.8. *continued* (c) Results from section 3 for primary isovels, secondary velocities and ADCP backscatter from September 1994. Only significant secondary velocities (> 0.15 m s^{-1}) are plotted

0 and 1440 m across the section and 103° between 1440 and 2000 m (Figure 25.8b). Compared to results for May, the area of flow bifurcation has remained in about the same location, but the angle of divergence between the flow streams has increased from 18 to 25°. The cross-section is no longer parabolic, but exhibits a pronounced medial bar (1100 to 1400 m) separating talwegs at 1000 and 1750 m across the transect.

The primary velocity isovels again show two high-velocity filaments, associated with flows heading towards the left and right sub-channels, but the high-velocity stream in the right sub-channel has expanded noticeably compared to May. The secondary flow pattern has changed radically. Clockwise helical flow is now present in the right flow stream, while flow in the left channel is directed to the west over in the upper portion of the section with strong vertical velocities associated with the complex bed features (800 to 1440 m in Figure 25.8b). It appears that the skew induced cell from the bend upstream has migrated westwards and that water is being drawn across the line of flow bifurcation from the diminishing left channel into the growing right channel. At this high stage, a relatively small back channel along the left bank (0 to 250 m) contains significant flow, which is following a path that is hydraulically separated from the rest of the cross-section by a wide, shallow shelf (250 to 750 m).

The backscatter plot for August shows low sediment concentration associated with the clockwise helical cell in the right sub-channel (1600 to 1800 m) and an area of high sediment concentration above the medial bar (1100 to 1400 m) where near-bed secondary components converge. The shape of the bed on the medial bar suggests that climbing dunes may be present on the gently sloping stoss (east) flank due to strong secondary flow from left to right over the bar.

The bed level change plot for the period May to August at section 3 (Figure 25.9a) illustrates the building of a medial bar with climbing dunes. Erosion is evident in the sub-channels on either side, but is most pronounced in the right sub-channel which exhibits both bed scour and bank retreat. This pattern of morphological development is consistent with the observed westward (rightwards) migration of the clockwise-rotating secondary cell, acceleration of primary flow in the right sub-channel and bed sedimentation where water crossing the bar from the diminishing left sub-channel meets an area of upwelling due to helical flow in the right sub-channel, to produce near-bed convergence.

The results for September are shown in Figure 25.8c. The procedure to locate the primary and secondary planes for this section again reveals two primary directions in the flow field, with headings of 88° for the flow between 0 and 417 m across the section and 114° between 417 and 963 m across (Figure 25.8c). That is, the flow in the left sub-channel has ceased to swing to the east, but has swung back towards the west, while flow in the right sub-channel has continued to veer west. As a result the angle of divergence has remained approximately constant at 26°. Falling stages on the recession of the monsoon flood restricts flow to the main channel, making it impossible to navigate over the shelf that was covered in August (0 to

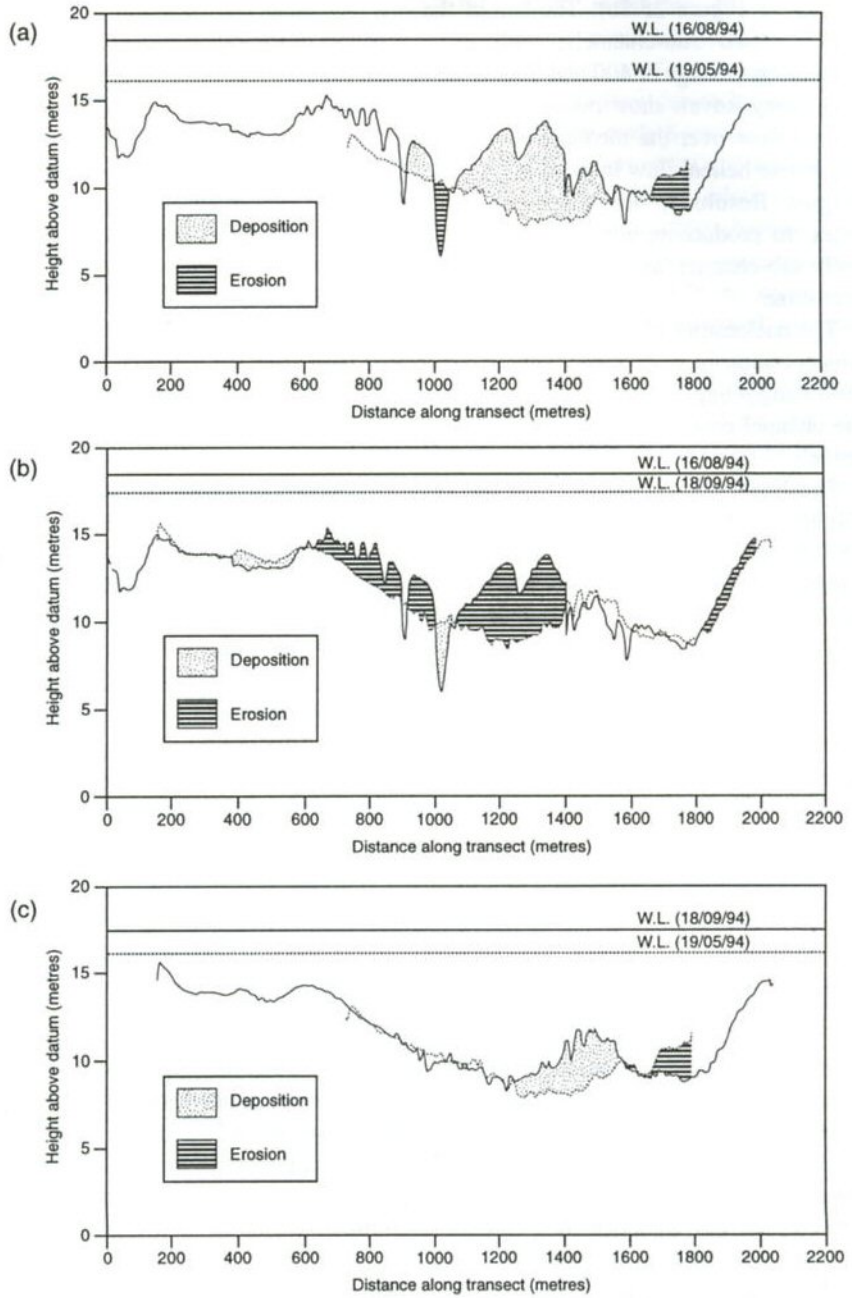

Figure 25.9. Bed level changes at section 3 between (a) May and August; (b) August and September; and (c) May and September 1994

800 m in Figure 25.8b). The bed in the main channel cross-section now clearly displays two sub-channels, with a pronounced medial bar (250 to 500 m) separating talwegs at 100 and 700 m across the transect in Figure 25.8c.

Primary isovels show two well-defined velocity maxima, separated by an area of slower flow over the medial bar. Secondary velocities indicate persistence of the clockwise helical flow in the right sub-channel that was identified in the results for August. Results for the left sub-channel are clearer and display an anticlockwise helix, to produce an almost symmetrical pattern with surface flow divergence in each sub-channel and secondary flow convergence over the medial bar at the centreline.

The backscatter plot in Figure 25.8c reveals filaments of relatively low sediment concentration in both sub-channels, associated with the two mirrored helical cells producing plunging flow near the banks. Sediment concentrations are high around the channel centreline, above the medial bar, where secondary flows converge and upwell.

The bed-level change plot for the period August to September at section 3 (Figure 25.9b) illustrates that during the falling stage general scour has occurred, smoothing the bed profile. The large climbing dune bedforms built on the rising limb have been destroyed and the area of deep scour channel in the left sub-channel (at 1000 m in Figure 25.9a) has been filled. Significant erosion of the right bank, first evident in Figure 25.9a, has continued. The pattern of morphological development is consistent with the observation that the height of bedforms scales on the flow depth and intensity, both of which have diminished. Continued westward (rightwards) migration of the main helical secondary cell is evident and there appears to have been development of a clockwise, skew-induced cell in the left sub-channel due to flow curvature around the growing medial bar at about the channel centreline. Erosion on the right margin drives enlargement of the right sub-channel that is associated directly with the change in dominance between the two sub-channels discussed earlier.

PRELIMINARY CONCLUSIONS

The ADCP measurements taken at section 6 indicate that cross-sectional morphology, primary isovels, secondary flows and suspended sediment distributions in bends of braided rivers share some common features with patterns observed in meander bends of single-thread rivers. The results support the hypothetical flow and cross-sectional distributions shown in Figure 25.2b. These findings suggest that elements of our understanding of process-form interactions in meandering rivers may be transferable to braided rivers.

The results for section 3 illustrate how hydraulic bifurcation of the flow affects the distributions of primary velocity, secondary flow and sediment concentration and drives morphological changes by controlling the distribution of sediment

transport, erosion and deposition around the wetted perimeter. Measurements repeated during the rising, peak and falling limbs of the monsoon flood reveal that morphological change occurs as a result of the combination of stage-related scour and fill coupled with incremental shifting in the pattern of flow driven by evolution in the distribution and circulation of flow approaching the study Section.

Zones of relatively low sediment concentration in the plots of ADCP backscatter intensity correlate well with areas of erosion, while areas of relatively high concentration are associated with upwelling flow. The similarity between the sediment distributions recorded at section 6 in May 1994 and those measured using sediment samplers in meandering rivers suggests that the ADCP backscatter is capable of producing reliable, qualitative pictures of relative suspended sediment concentrations.

The main response of the channel to the imposed flow field during the 1994 monsoon flood was to enlarge the right sub-channel at the expense of the left sub-channel (Figure 25.9c). A medial bar grew along the channel centreline, where secondary flow converged. These changes may be explained in terms of the local flow patterns, but those patterns are themselves a product of planform evolution that has affected the orientation and curvature of flow approaching the study site. Historical satellite images (Figure 25.6) show that a bend cut-off upstream led to a change in flow heading and a reversal of planform curvature in the flow approaching the bifurcation. Strong, clockwise helical flow generated by a right-bank concave bend upstream of the bifurcation at the study site dominated flow patterns at section 3 and led directly to erosion at the right margin and deposition at the channel centre. Hence, it must be concluded that channel changes in the study area can only be explained when observed flow and sediment processes are viewed within the context of morphological changes at larger spatial and temporal scales.

ACKNOWLEDGEMENTS

Financial support for this study was provided by the Engineering and Physical Sciences Research Council (UK) through a CASE studentship (B/93561631) with Sir William Halcrow & Partners Ltd. The study was performed as part of a joint project between the University of Nottingham, Delft Hydraulics and the Danish Hydraulics Institute. Technical and logistical support were provided by all the staff and advisers at FAP-24, River Survey Project in Bangladesh. Particular thanks go to Hans Høyer, Pieter van Groen, Johan Grijsen, and Project Adviser J.J. Peters.

REFERENCES

Ashworth, P.J., Ferguson R.I. & Powell, M.D. 1992. 'Bedload transport and sorting in braided channels', in Billi, P., Hey, R.D., Thorne, C.R. & Tacconi, P. (Eds) *Dynamics of Gravel Bed Rivers*, John Wiley & Sons Ltd., Chichester, 497–513.

Barua, D.K. 1994. 'On the environmental controls of Bangladesh river systems', *Asia Pacific J. Environment Development*, Bangladesh Unnayan Parishad (BUP), **1**, 81–98.

Bathurst, J.C. 1979. 'Distribution of boundary shear stress in rivers', in Rhodes, D.D. & Williams, G.P. (Eds) *Adjustments of the Fluvial System*, Kendall/Hunt Publishing Co, Dubuque, Iowa, 95–116.

Bathurst, J.C., Thorne, C.R. & Hey, R.D. 1977. 'Direct measurements of secondary currents in river bends', *Nature*, **269**, 504–506.

Bathurst, J.C., Thorne, C.R. & Hey, R.D. 1979. 'Secondary flow and shear stress at bends', *J. Hydraul. Div., ASCE*, **105**, 1277–1295.

Brammer, H. 1990. 'Floods in Bangladesh, geographical background to the 1987 and 1988 floods', *Geogr. Journal*, **156**, 12–22.

Bridge, J.S. 1977. 'Flow, bed topography, grain size and sedimentary structure in open-channel bends: a three-dimensional model', *Earth Surf. Processes*, **2**, 401–416.

Bridge, J.S. 1984. 'Flow and sedimentary process in river bends; comparison of field observations and theory', in Elliot, C.M. (Ed) *River Meandering*, ASCE, New York, 857–872.

Bridge, J.S. & Gabel, S.L. 1992. 'Flow and sediment dynamics in a low sinuosity river: Calamus River, Nebraska Sandhills', *Sedimentology*, **39**, 125–142.

Bristow, C.S. 1987. 'Brahmaputra River: channel migration and deposition', in Ethridge, F.G., Flores, R.M. and Harvey, M.D. (Eds) *Recent Developments in Fluvial Sedimentology*, Soc. Econ. Paleon. and Mineralogists, Sp. Pub. **39**, 63–74.

Bristow, C.S. & Best, J.L. 1993. 'Braided rivers: perspectives and problems', in Best, J.L. & Bristow, C.S. (Eds) *Braided Rivers*, Geol. Soc. London Sp. Pub., **75**, 1–11.

Coleman, J.M. 1969. 'Brahmaputra River: channel processes and sedimentation', *Sediment. Geol.*, **3**, 129–239.

Dietrich, W.E. 1982. *Flow, Boundary Shear Stress and Sediment Transport in a River Meander*, Unpub. PhD Diss., Univ. Washington at Seattle, 261 pp.

Dietrich, W.E. & Smith, J.D. 1983. 'Influence of the point bar on flow through curved channels', *Water Resour. Res.*, **19**, 1173–1192.

Dietrich, W.E., Smith, J.D. & Dunne, T. 1979. 'Flow and sediment transport in a sand-bedded meander', *J. Geol.*, **87**, 305–315.

Dietrich, W.E. & Whiting, P. 1989. 'Boundary shear stress and sediment transport in river meanders of sand and gravel', in Ikeda, S. & Parker, G. (Eds) *River Meandering*, AGU, Water Resources Monograph **12**, Washington, 1–50.

Engelund, F. 1974. 'Flow and bed topography in channel bends', *J. Hydraul. Div., ASCE*, **100**, 1631–1648.

Friedkin, J.F. 1945. *A Laboratory Study of the Meandering of Alluvial Rivers*, USACE Waterways Experiment Station, 40 pp.

Hey, R.D. & Thorne, C.R. 1975. 'Secondary Flows in River Channels', *Area*, **7**, 191–196.

Hey, R.D. & Thorne, C.R. 1975. 'Secondary Flows in River Channels – discussion', *Area*, **8**, 235–236

Klaassen, G.J. & van Zanten, B.H.J. 1989. 'On cut off ratios of curved channels', *Proc. 23rd Congr. IAHR*, Ottawa, 111–122. (also Delft Hydraul. Pub. No.444).

Lapointe, M.F. & Carson, M.A. 1986. 'Migration patterns of an asymmetrical meandering river: The Rouge River, Quebec', *Water Resour. Res.*, **22**, 731–743.

Leopold & Wolman, 1957. 'River channel patterns: braided, meandering and straight', *US Geol. Surv. Prof. Paper*, **282b**, 39–85.

Markham, A.J. & Thorne, C.R. 1992. 'Geomorphology of gravel bed river bends', in Billi, P., Hey, R.D., Thorne, C.R. & Tacconi, P. (Eds) *Dynamics of Grave-bed Rivers*, John Wiley & Sons Ltd., Chichester, 433–450.

McLelland, S.J., Ashworth, P.J. & Best, J.L. 1994. *Velocity Correction Methods in Open Channels: Description, Critique & Recommendations*, FAP-24 Working Paper, August 1994, 16 pp.

Odgaard, A.J. 1986. 'Meander flow model. II: Applications', *J. Hydraul. Engrg.*, **112**, 1137–1150.

Odgaard, A.J. & Bergs, M.A. 1988 'Flow processes in a curved alluvial channel', *Water Resour. Res.*, **24**, 45–56.

Perkins, H.J. 1970. 'The formation of streamwise vorticity in turbulent flow', *J. Fluid Mech.*, **44**, 721–740.

Peters, J.J. 1977. 'Sediment transport in the Zaire River', in Nihoul, J.C.J. (Ed) *Bottom Turbulence, Proc. 8th Int. Liege Colloq. on Ocean Dynamics*, **19**, 221–236.

Peters, J.J. & Goldberg, A. 1989. 'Flow data in large alluvial channels', in Maksimovic, C. & Radojkovic, M. (Eds) *Computational Modelling and Experimental Methods in Hydraulics,* (Hydrocomp 1989), Elsevier, London, 77–86.

Prandtl, L. 1952. *Essentials of Fluid Dynamics,* Blackie, London, 452 pp.

Smith, J.D. & McLean, S.R. 1984. 'A model for meandering streams', *Water Resour. Res.*, **20**, 1301–1315.

Thorne, C.R. & Hey, R.D. 1979. 'Direct measurements of secondary currents at a river inflexion point', *Nature*, **280**, 226–228.

Thorne, C.R. & Lewin, J. 1979. 'Bank processes, bed material movement and planform development in a meandering river', in Rhodes, D.D. & Williams, G.P. (Eds) *Adjustments of the Fluvial System*, Kendall/Hunt Publishing Co, Dubuque, Iowa, 117–137.

Thorne, C.R & Rias, S. 1984. 'Secondary current measurements in a meandering river', in *River Meanders*, ASCE Sp. Pub., Proc. Rivers '83, ASCE Publications, 675–686.

Thorne, C.R. & Richardson, W.R.R. 1995. *Secondary Current Measurements Around a Bar in the Brahmaputra River, Bangladesh*, Draft Final Report to FAP-24, Univ. of Nottingham, 65 pp.

Thorne, C.R., Russell, A.P.G. & Alam, M.K. 1993. 'Planform pattern and channel evolution of the Brahmaputra River, Bangladesh', in Best, J.L. & Bristow, C.S. (Eds) *Braided Rivers*, Geol. Soc. London Sp. Pub., **75**, 257–276.

Thorne, C.R., Zevenbergen, L.W., Pitlick, J.C., Rais, S., Bradley, J.B. & Julien, P.Y. 1985. 'Direct measurements of secondary currents in a meandering sand-bed river', *Nature*, **316**, 746–747.

Thorne, P.D., Hardcastle, P.J., Flatt, D. & Humphery, J.D. 1994. 'On the use of acoustics for measuring shallow water suspended sediment processes', *IEEE J. Oceanic Engrg.*, **19**, 48–57.

NOTATION

U_P	primary velocity component
U_S	secondary velocity component
V_H	resultant velocity in the horizontal plane
W	width of the measurement ensemble
y	depth of measurement 'bin'
Y	average depth
α	flow orientation
φ	velocity direction